Journal of Autoimmunity 100 (2019) 84–94

Contents lists available at ScienceDirect

Journal of Autoimmunity

journal homepage: www.elsevier.com/locate/jautimm

cGAS activation causes lupus-like autoimmune disorders in a TREX1 mutant mouse model

Nanyang Xiao[a], Jingjing Wei[a], Shan Xu[a], Hekang Du[a], Miaohui Huang[a], Sitong Zhang[a], Weiwei Ye[a], Lijun Sun[a,b,**], Qi Chen[a,*]

[a] Fujian Key Laboratory of Innate Immune Biology, Biomedical Research Center of South China, College of Life Science, Fujian Normal University, Fuzhou, Fujian, 350117, China

[b] Department of Molecular Biology, University of Texas Southwestern Medical Center, Dallas, TX 75390-9148, USA

ARTICLE INFO

Keywords:
Autoimmune disorder
Trex1 mutation
Innate immunity
cGAS
Lupus
DNA sensor
IFN-signature

ABSTRACT

TREX1 encodes a major cellular DNA exonuclease. Mutations of this gene in human cause cellular accumulation of DNA that triggers autoimmune diseases including Aicardi–Goutieres Syndrome (AGS) and systemic lupus erythematosus (SLE). We created a lupus mouse model by engineering a D18 N mutation in the *Trex1* gene which inactivates the enzyme and has been found in human patients with lupus-like disorders. The $Trex1^{D18N/D18N}$ mice exhibited systemic inflammation that consistently recapitulates many characteristics of human AGS and SLE. Importantly, ablation of *cGas* gene in the $Trex1^{D18N/D18N}$ mice rescued the lethality and all detectable pathological phenotypes, including multi-organ inflammation, interferon stimulated gene induction, autoantibody production and aberrant T-cell activation. These results indicate that cGAS is a key mediator in the autoimmune disease associated with defective TREX1 function, providing additional insights into disease pathogenesis and guidance to the development of therapeutics for human systemic autoimmune disorders.

1. Introduction

As the first line of defense mechanism, the innate immune system develops pattern-recognition receptors (PRRs) to recognize invading pathogens. PRRs detect pathogen-associated molecular patterns (PAMPs) and initiate immune responses to protect the host from infection and other diseases. Nucleic Acids, the key components for microbial replication and propagation, can be recognized as PAMP by the Toll-like receptor family (TLRs) and cytosolic sensors for RNA and DNA [1–3]. As genetic material, DNA is usually confined to cellular compartments such as nuclei and mitochondria. When DNA is present in the cytoplasm, it becomes a PAMP that can elicit immune response. Cyclic GMP-AMP synthase (cGAS) is a major sensor that detects cytoplasmic DNA [4,5]. Binding to DNA triggers enzymatic activation of cGAS, which utilizes ATP and GTP to synthesize cyclic GMP-AMP (cGAMP). As a second messenger, cGAMP binds to and activate the ER adapter protein Stimulator of Interferon Genes (STING) [4], which leads to sequential activation of kinase complexes including TBK1 and IKK, transcription factors IRF3/IRF7 and NF-κB, and expression of type I interferons and inflammatory cytokines [4–6]. In parallel, microbe-generated RNA species in the cytoplasm are detected by retinoic acid inducible gene-I (RIG-I) and melanoma differentiation associated gene 5 (MDA5), which interact with the mitochondrial antiviral signaling protein (MAVS) to activate TBK1 and IKK, and downstream signaling events [7].

When cells are not under attack by microbes, the cytoplasm is largely free of DNA in part through the action of several deoxyribonuclease (DNases), such as TREX1 [8]. TREX1 is a major cytoplasmic exonuclease that degrades dsDNA and ssDNA [9,10]. Loss-of-function mutations in the human *TREX1* gene have been linked to a spectrum of autoimmune diseases, including the Aicardi-Goutieres syndrome (AGS), a severe neuroinflammatory disorder, the familial chilblain lupus (FCL), a monogenic form of cutaneous lupus erythematosus, the systemic lupus erythematosus (SLE), and the retinal vasculopathy and cerebral leukodystrophy (RVCL) [11–13]. A common feature of these TREX1-associated autoimmune diseases is the elevated expression of type I interferons and interferon-stimulated genes (ISGs) [14–16], suggesting that the failure to clear cytosolic DNA drives the interferon pathway. Mice lacking the *Trex1* gene display shortened lifespan, multi-organ inflammation, and autoantibodies [17]. These autoimmune symptoms

* Corresponding author. Fujian Key Laboratory of Innate Immune Biology, Biomedical Research Center of South China, College of Life Science, Fujian Normal University, Fuzhou, Fujian, 350117, China.

** Corresponding author. Department of Molecular Biology, University of Texas Southwestern Medical Center, Dallas, TX 75390-9148, USA.

E-mail addresses: lijun.sun@utsouthwestern.edu (L. Sun), chenqi@fjnu.edu.cn (Q. Chen).

https://doi.org/10.1016/j.jaut.2019.03.001
Received 25 January 2019; Received in revised form 1 March 2019; Accepted 4 March 2019
Available online 11 March 2019

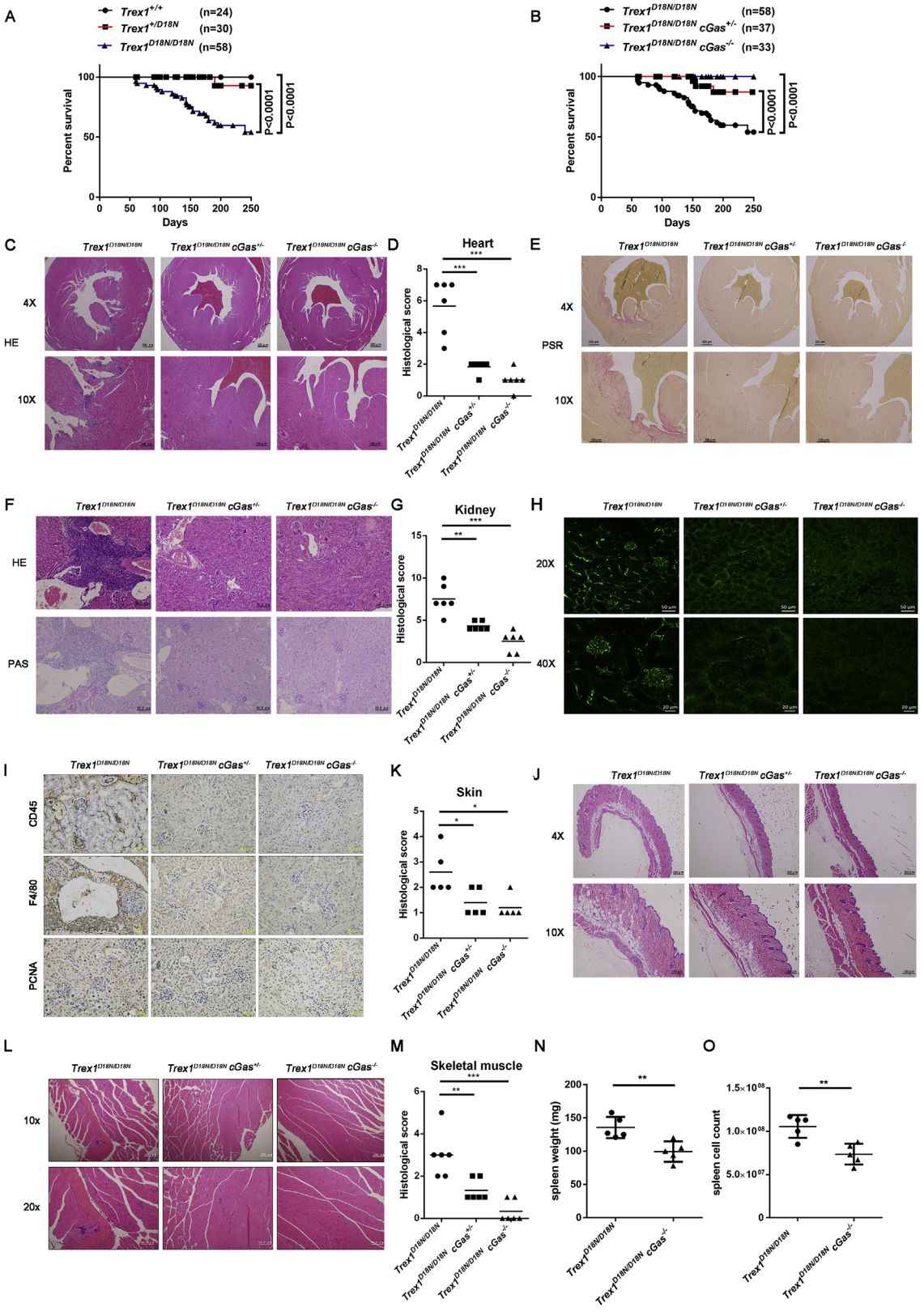

(caption on next page)

can be rescued by simultaneous deletion of *cGAS* gene [18,19]. To better recapitulate disease phenotype in humans, mice carrying the same disease-causing mutations in human *TREX1* gene will provide an improved platform to study disease mechanism and to develop therapeutic interventions. D18 N is such a mutation that is present in autoimmune patients [13]. *Trex1* D18 N mutant in mice is expressed normally but is defective in digesting ssDNA and nicked dsDNA [20]. Mice carrying D18 N mutation exhibit systemic inflammation, lymphoid hyperplasia, vasculitis, and kidney disease [20,21]. However, the role of DNA sensing pathway in causing autoimmune phenotype in

Fig. 1. cGAS causes the lethality and lupus-like inflammation in multiple organs of *Trex1*$^{D18N/D18N}$ mice. (A) Survival curves of *Trex1*$^{+/+}$, *Trex1*$^{+/D18N}$ and *Trex1*$^{D18N/D18N}$ mice. **(B)** Survival curves of *Trex1*$^{D18N/D18N}$, *Trex1*$^{D18N/D18N}$ *cGas* $^{\pm}$ and *Trex1*$^{D18N/D18N}$ *cGas*$^{-/-}$ mice. Statistical analyses in A and B were performed with the Log-rank (Mantel-Cox) test. (**C**) H&E staining of the hearts from mice of indicated genotypes. (**D**) Blinded histological analysis of the hearts from indicated mice. (**E**) Periodic Acid Schiff (PAS)-staining of the hearts from indicated mice. (**F**) H&E and PAS staining of the kidney sections from indicated mice. (**G**) Blinded histological analysis of the kidneys from indicated mice. (**H**) Immunofluorescence staining for IgG in the kidney sections from indicated mice. (**I**) The kidney sections from indicated mice were stained with anti-CD45, *anti*-F4/80, and *anti*-PCNA antibodies. (**J**) H&E staining of the skin from mice of indicated genotypes. (**K**) Histological scoring of the skin from indicated mice. (**L**) H&E staining of the skeletal muscle from mice of indicated genotypes (**M**) Histological scoring of the skeletal muscle from indicated mice. Statistics of histological scores were performed using Student's *t*-test. *: $p < 0.05$, **: $p < 0.01$, ***: $p < 0.001$, ****: $p < 0.0001$. (**N**) Spleen weight and (**O**) Splenocyte cell counts were measured from 4-month mice as indicated. The error bars represent the mean and SD. Statistical analysis was performed with a two-tailed *t*-test. **: $p < 0.01$.

these mice has not been investigated.

We independently generated mice harboring D18 N mutation of *Trex1* gene using the CRISPR/Cas9 technology. The *Trex1*$^{D18N/D18N}$ mice manifest autoimmune symptoms that consistently recapitulate many characteristics of human familial chilblain lupus. By further deleting *cGas* gene in *Trex1*$^{D18N/D18N}$ mice, we demonstrated the essential role of cGAS in mediating these disease phenotypes. This study confirmed the role of cGAS in linking a specific gene mutation to an autoimmune disease, and provided a better platform for testing novel therapeutic interventions.

2. Results

2.1. cGAS is responsible for lethal autoimmunity disease in Trex1D18 N mice

To characterize the disease phenotype caused by D18 N mutation in the *Trex1* gene and determine the role of cGAS in this autoimmune mouse model, we generated *Trex1*^{D18N} mice by targeted knock-in of the mutant allele using the CRISPR/Cas9 system (Figs. S1A and S1B). This mouse line was on C57BL/6J background rather than the 129S6/SvEvTac background [20], which has a predisposition to the lupus disease [22]. TREX1-D18 N mutant is orthologous to the pathogenic mutation identified in patients with FCL and SLE [20,23,24]. Western blotting data showed normal expression of the TREX1 D18 N protein in *Trex1*$^{WT/D18N}$ and *Trex1*$^{D18N/D18N}$ mice compared to wild type mice (Fig. S1J). *Trex1*$^{WT/D18N}$ heterozygous mice didn't exhibit noticeable unhealthy conditions, consistent with the lack of detectable cytoplasmic dsDNA in MEFs as shown by immunofluorescence staining (Fig. S6A). Like the *Trex1*$^{-/-}$ mice and consistent with other studies [20], *Trex1*$^{D18N/D18N}$ mice exhibited shortened life span, but less severe phenotypes than *Trex1*$^{-/-}$ mice. Although *Trex1*$^{D18N/D18N}$ mice start dying at average age of 8 weeks, greater than 50% of mice can survive over 25 weeks. In addition, *Trex1*$^{D18N/D18N}$ mice are fertile up to 6 months.

To determine whether the premature death phenotype of *Trex1*D18 N mice was caused by cGAS activation in response to abnormal intracellular DNA accumulation due to loss of function of the mutant TREX1 enzyme, we further deleted *cGas* gene from *Trex1*$^{D18N/D18N}$ mice by breeding. Deletion of both alleles of *cGas* gene completely rescued survival of *Trex1*$^{D18N/D18N}$ mice; more strikingly, deletion of one allele of *cGas* rescued majority of mice from early death (Fig. 1B). Histological analysis revealed inflammation in multiple organs of *Trex1*D18 N mice including heart, kidney, and skin (Figs. S1C–I). Inflammatory myocarditis and fibrosis were obvious in the heart; IgG deposit and increased infiltrating CD45^{+} cells and F4/80 + macrophages in the glomeruli was observed in kidney sections (Fig. 1I). In addition, *Trex1*$^{D18N/D18N}$ mice had enlarged spleens and increased numbers of splenocytes (Fig. 1N and O). All these autoimmune phenotypes were completely eliminated in *Trex1*$^{D18N/D18N}$ *cGas*$^{-/-}$ mice (Fig. 1), as indicated by organ sections and accompanied by double-blinded histological scoring. Again, deleting just one allele of *cGas* was sufficient to markedly reduce disease phenotypes including heart and kidney inflammation, indicating cGAS mediates the development of autoimmune disease and lethality in *Trex1*$^{D18N/D18N}$ mice.

2.2. cGAS promotes upregulation of ISGs and inflammatory cytokines in TREX1-D18 N mice

Since type I interferon response and upregulation of ISGs and inflammatory genes are important indicators of autoimmunity in human patients, we next examined the molecular signatures of immune activation in *Trex1*$^{D18N/D18N}$ mice. As revealed by quantitative RT-PCR, elevated levels of ISGs including Cxcl10, ISG15, IFIT1, OAS1, Ccl5, as well as inflammatory genes such as IL12p40 were observed in the hearts and kidneys of *Trex1*-D18 N mice, compared to their wild-type littermates (Figs. S2A and S2B). To characterize the change in gene expression profile caused by D18 N mutation in *Trex1* gene, we performed RNA seq analysis in mouse embryonic fibroblasts (MEFs). D18 N mutation on both alleles of *Trex1* led to > 2-fold upregulation of more than 400 genes (Fig. S2C and supplementary RNA-seq data), the majority of which belongs to the category of “immune response” (Fig. S2E). A number of upregulated genes including interferon-β and a few ISGs were confirmed by quantitative RT-PCR (Fig. S2D). D18 N mutation in a single allele of *Trex1* gene didn't cause obvious elevation of these genes. When *cGas* gene was deleted from *Trex1*$^{D18N/D18N}$ mice, upregulation of these ISGs and inflammatory genes was largely abolished in the heart, kidney, PBMC, and MEFs (Fig. 2A–D). Deletion of one *cGas* allele was able to markedly reduce expression levels of these genes. These results indicate upregulation of ISGs and inflammatory genes was mediated by cGAS in *Trex1*$^{D18N/D18N}$ autoimmune mice.

2.3. cGAS is responsible for the autoantibody production in Trex1 mutant mice

Autoantibodies production is one of the hallmarks of lupus-like autoimmunity. *Trex1*$^{D18N/D18N}$ mice, but not *Trex1*$^{WT/D18N}$ mice developed antibodies against nuclear antigens (ANA, Fig. S3C). Further analyses reveal the presence of autoantibodies against ssDNA, dsDNA, and nuclear proteins such as Histone 3 and U1 subunit of small nuclear ribonucleoprotein (U1-snRNP) (Figs. S3A, S3B, S3D, and S3E). Anti-IL12 antibody was also elevated (Fig. S3F). Ablation of both alleles of *cGas* gene in *Trex1*D18 N mice abolished autoantibody production (Fig. 3). Deletion of one allele of *cGas* largely reduced autoantibody levels. These findings confirmed cGAS is responsible for autoantibody response in lupus-like diseases.

2.4. cGAS is essential for the hyperactive T cells in Trex1 mutant mice

Spontaneous T cell activation plays an important role during autoimmune responses [25]. To verify the mechanism of *Trex1* mutation-caused autoimmune phenotype, we first evaluated T cell activity in *Trex1*$^{D18N/D18N}$ mice. We observed enhanced CD69 levels on the surface of CD4 and CD8 T cells and increased Ly6c levels on CD8 T cells, indicating the hyperactive T cells were produced in *Trex1*$^{D18N/D18N}$ mice (Figs. S4A, B, C). However, these increases in active T cells were abolished in *Trex1*$^{D18N/D18N}$-*cGas*$^{+/-}$ and *Trex1*$^{D18N/D18N}$-*cGas*$^{-/-}$ mice (Fig. 4A–C). In addition, our data indicated that the elevated levels of CD4 and CD8 memory T cells (CD44^{hi}/CD62L^{lo}) in *Trex1*$^{D18N/D18N}$ were also markedly reduced by the deletion of *cGas* gene (Figs. S4D and E and Fig. 4D and E).

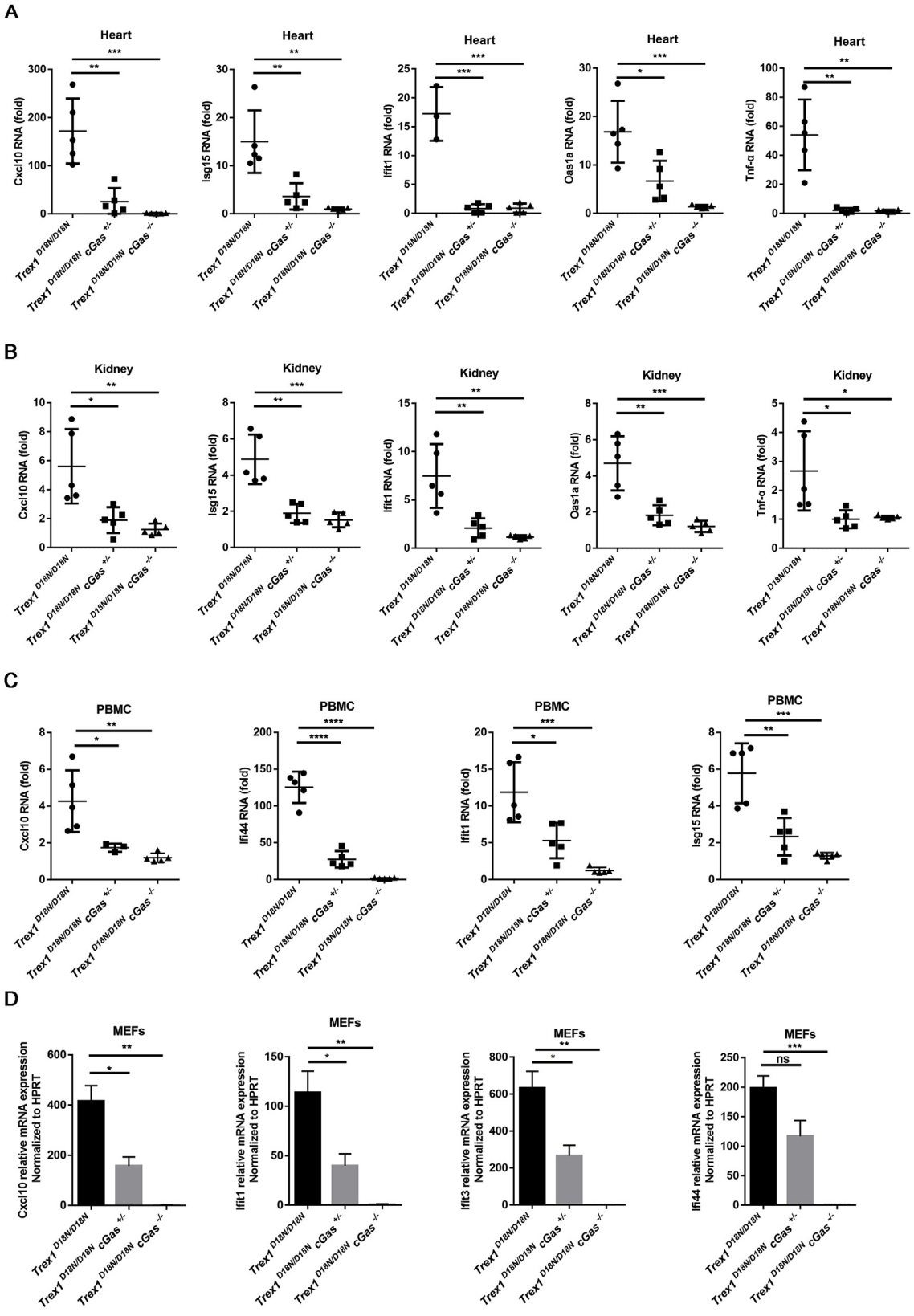

Fig. 2. cGAS induces the increased ISGs expression in *Trex1*$^{D18N/D18N}$ mice. Quantitative RT-PCR analysis of ISGs and TNFα mRNA in the hearts (**A**), kidneys (**B**), PBMC (**C**) and MEFs (**D**) from *Trex1*$^{D18N/D18N}$, *Trex1*$^{D18N/D18N}$ *cGas* $^{\pm}$ and *Trex1*$^{D18N/D18N}$ *cGas*$^{-/-}$ mice. Statistics were performed using Student's *t*-test. *: $p < 0.05$, **: $p < 0.01$, ***: $p < 0.001$, ****: $p < 0.0001$.

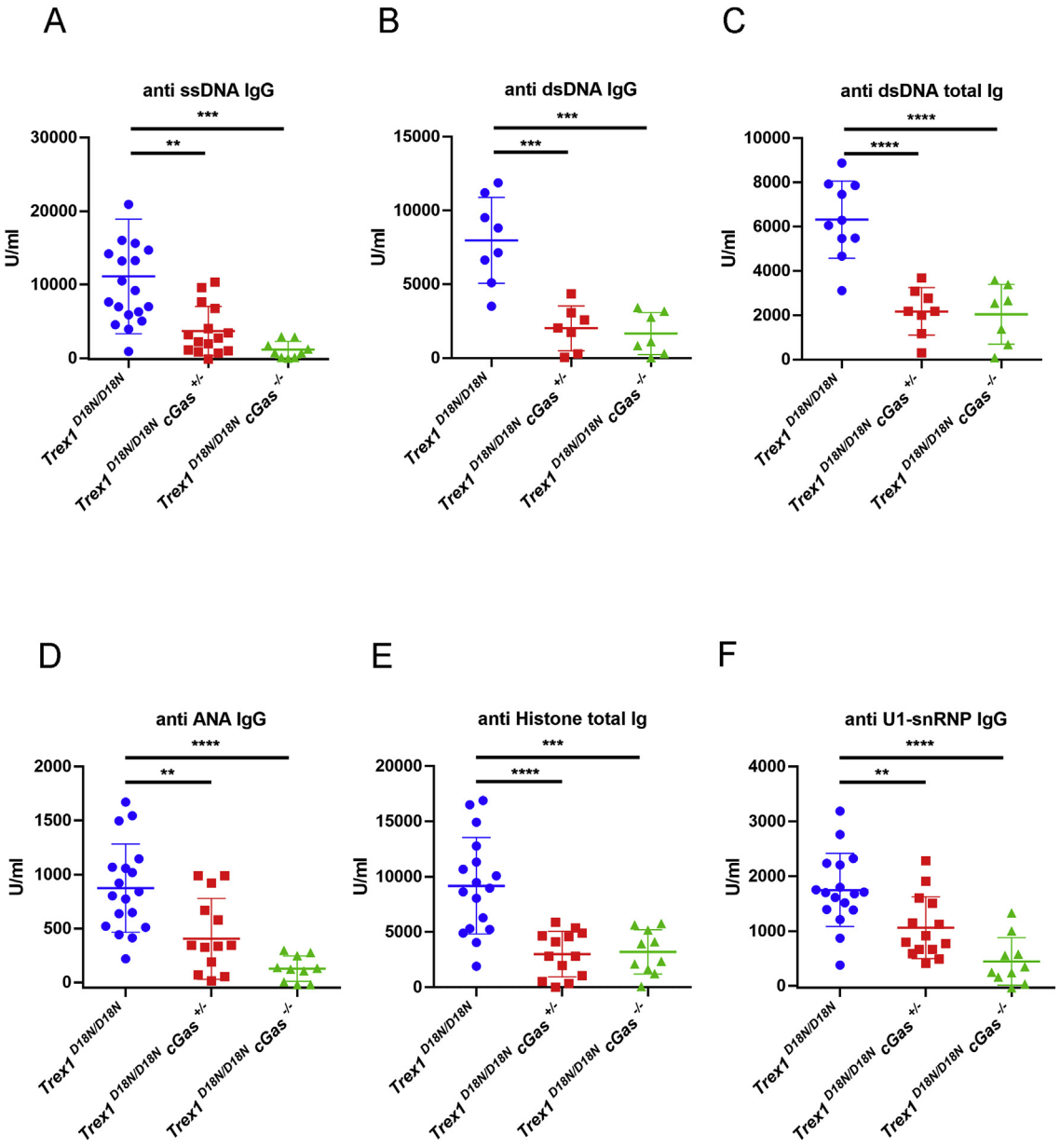

Fig. 3. cGAS is required for generation of autoantibodies in *Trex1*$^{D18N/D18N}$ mice. ELISA quantification of autoantibodies in sera from *Trex1*$^{D18N/D18N}$, *Trex1*$^{D18N/D18N}$ *cGas* $^{\pm}$ and *Trex1*$^{D18N/D18N}$ *cGas*$^{-/-}$mice. (**A**) ssDNA IgG, (**B**) dsDNA IgG, (**C**) dsDNA Ig's (total A + G + M), (**D**) Antinuclear antibody (ANA), (**E**) Anti-Histone Ig's(total A + G + M), and (**F**) Anti-small nuclear ribonucleoproteins (sn-RNP) IgG. Statistics were performed using Student's *t*-test. *: $p < 0.05$, **: $p < 0.01$, ***: $p < 0.001$, ****: $p < 0.0001$.

To evaluate T cell activation, we stimulated these cells from mice of different genotypes with PMA and measured levels of T-bet and Interferon-γ (IFN-γ). D18 N mutation in *Trex1* gene caused elevated expression of IFN-γ in both CD4 and CD8 T cells from spleen (Figs. S5A and S5B) and PBMC samples (Figs. S5C and S5D), indicating these T cells are hyper-reactive. High expression levels of T-bet and IFN-γ were greatly reduced in CD4 and CD8 T cells from spleen and PBMC of *Trex1*$^{D18N/D18N}$-*cGas*$^{+/-}$ and *Trex1*$^{D18N/D18N}$-*cGas*$^{-/-}$ mice (Fig. 5A–E). Furthermore, the elevated expression of IFN-γ (Fig. 6B), IL-12p40 (Fig. 6D), as well as Tbx21 (Fig. 6F) was detected in the heart from *Trex1*$^{D18N/D18N}$ mice; however, these elevations were abolished when one or two alleles of *cGas* were deleted (Fig. 6A, C, and E), indicating infiltration of hyperactive T cells are involved in development of inflammatory myocarditis, which is medicated by cGAS. These findings further underline the role of cGAS in the development of lupus-like autoimmunity.

3. Discussion

TREX1 functions as a crucial DNase to protect the host innate immune system from excessive activation [26]. Multiple *TREX1* mutations have been identified in human patients with severe autoimmune and spontaneous inflammatory diseases [27–29]. Here, we established a *Trex1* missense mouse model to better simulate the clinical and pathologic features of the human disease than the previously constructed *Trex1*$^{-/-}$ mice. D18 N mutant, as found in familial chilblain lupus patients, affects a highly conserved amino acid residue critical for chelating Mg^{2+} ion and therefore essential for the catalytic activity of TREX1 [30]. TREX1-D18 N protein lost DNase activity toward both dsDNA and ssDNA [31]. The *Trex1*$^{D18N/D18N}$ mice develop similar autoimmune disease phenotypes, including inflammation in multiple tissues, elevated autoantibodies, hyperactive T cell, and typical interferon-signaling signature. Interestingly, these autoimmune phenotypes

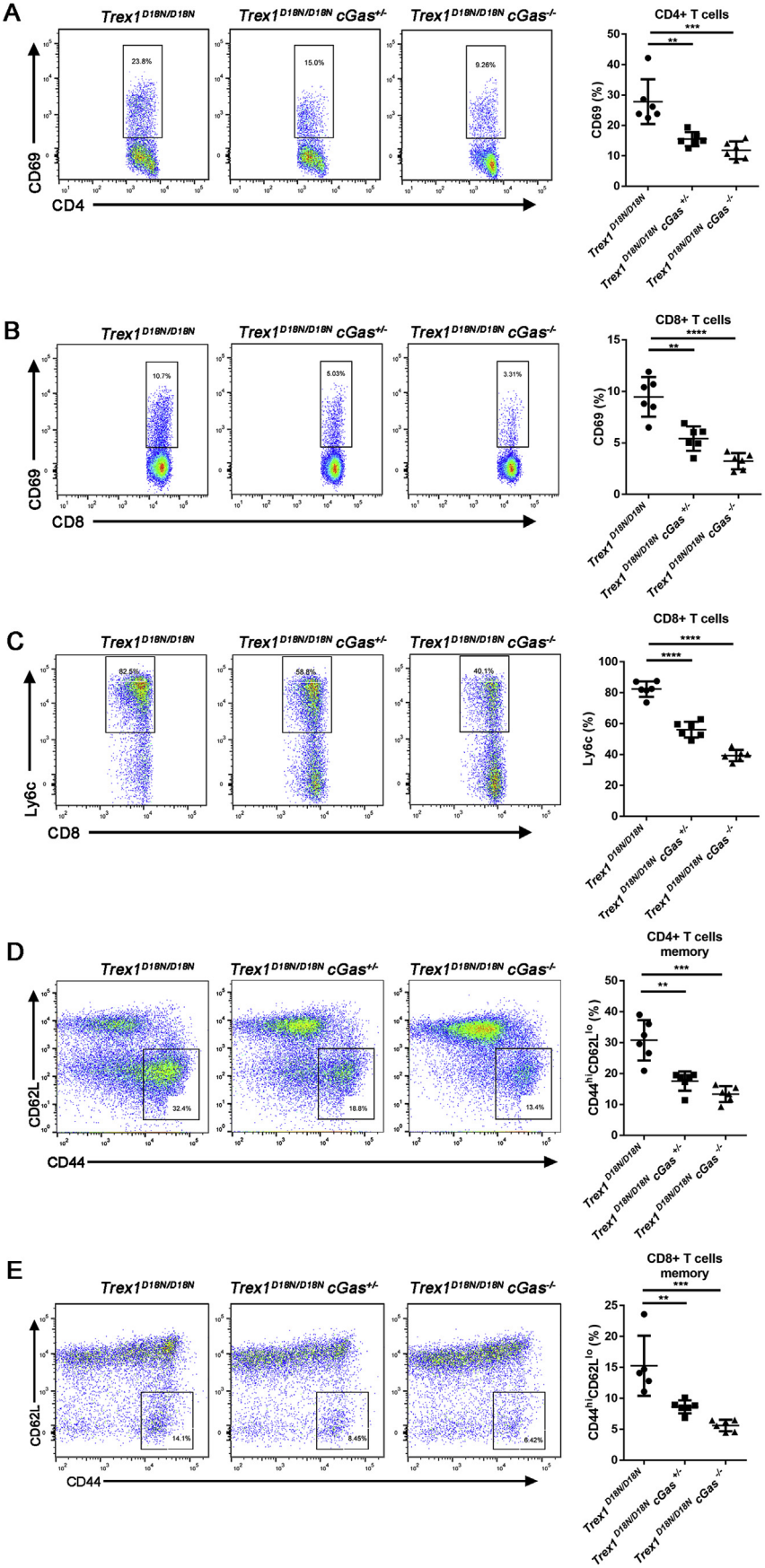

Fig. 4. cGAS drives T cells activation in *Trex1*$^{D18N/D18N}$ mice. Representative Flow-cytometric plots and quantification of the frequency of (**A**) activated CD4$^+$ T cells, (**B**) activated CD8$^+$ T cells, (**C**) Ly6c in CD8$^+$ T cells, (**D**)memory CD4$^+$ T cells, and (**E**) memory CD8$^+$ T cells in the spleen of *Trex1*$^{D18N/D18N}$, *Trex1*$^{D18N/D18N}$ *cGas* $^{\pm}$ and *Trex1*$^{D18N/D18N}$ *cGas*$^{-/-}$ mice. Error bars represent SD. *$p < 0.05$; **$p < 0.01$; ***$p < 0.001$; ****$p < 0.0001$, by unpaired Student's *t*-test.

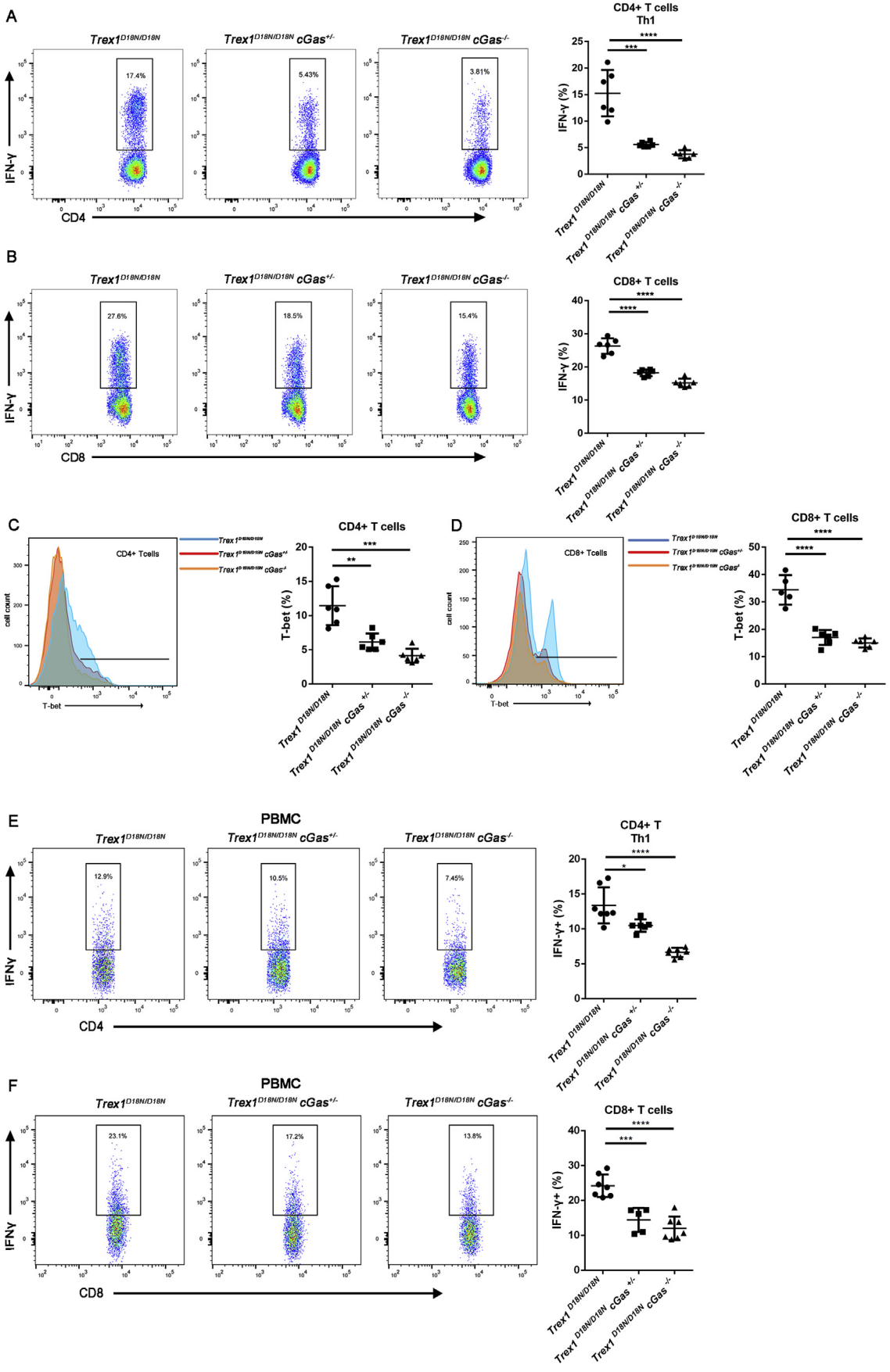

(caption on next page)

Fig. 5. cGAS is responsible for hyperreactive T cells generation in *Trex1*$^{D18N/D18N}$ mice. (**A** and **B**): Representative Flow-cytometric plots and quantification of the frequency of intracellular IFN-γ in response to PMA plus ionomycin treatment in splenic CD4$^+$ T cells (A) and CD8$^+$ T cells (B) from *Trex1*$^{D18N/D18N}$, *Trex1*$^{D18N/D18N}$ *cGas*$^{+/-}$ and *Trex1*$^{D18N/D18N}$ *cGas*$^{-/-}$ mice. (**C** and **D**) FACS analysis of T-bet levels in splenic CD4$^+$ (C) and CD8$^+$ (D) T cells from indicated genotypes. (**E** and **F**): Similar to (A–B), IFN-γ$^+$ CD4$^+$ T cells (E) and IFN-γ$^+$ CD8$^+$ T cells (F) in PBMC were analyzed. Error bars represent SD. *$p < 0.05$; **$p < 0.01$; ***$p < 0.001$; ****$p < 0.0001$, by unpaired Student's *t*-test.

were eliminated by genetic deletion of the DNA sensor cGAS. Our results suggest that cGAS is responsible for the lupus-like autoimmune diseases FCL caused by a *TREX1* missense mutation and confirm that cGAS-STING pathway activation is the key signaling for autoimmunity.

Trex1$^{D18N/D18N}$ mice exhibited less severe phenotype compared to *Trex1*$^{-/-}$ mice (our unpublished data and references 20,21). It is possible that TREX1 has functions that are independent of its DNase activity. TREX1 protein contains an N-terminal exonuclease domain and a C-terminal domain tailed with a single transmembrane motif that anchors to ER [32,33]. Frameshift mutations at C-terminals have been associated with autoimmune disorders such as RVCL [34]. In addition to localizing TREX1 protein to ER, the C-terminal of TREX1 may have DNase-independent functions. In a study, a chimeric protein with GFP replacing the N-terminal exonuclease domain of TREX1 was able to suppress ISG elevation when expressed in *Trex1*$^{-/-}$ cells [32]. It would be interesting to test whether this is true in mice. Nonetheless, *Trex1*$^{D18N/D18N}$ mice provided a more specific model to study the disease that is caused by the same missense mutation in human.

TREX1D18 N mutant exhibits dominant effects in human, actually only heterozygous D18 N mutation was found in human patients [12,24,31,35]. Therefore, it was a surprise to see *Trex1*$^{WT/D18N}$ mice exhibited no overt phenotype. Biochemical studies have demonstrated TREX1 WT/D18 N heterodimer protein was not able to digest dsDNA. However, in *Trex1*$^{WT/D18N}$ cells, it is reasonable that active WT/WT homodimers will exist in a certain proportion. Whether these functional homodimers have access to dsDNA that are locked and protected by D18 N homodimers or WT/D18 N heterodimers remains a question, but our data indicate MEFs from *Trex1*$^{WT/D18N}$ mice are devoid of detectible dsDNA in their cytoplasm (Fig. S6A), suggesting these mice have functional TREX1 enzymes, which are likely WT/WT homodimers. To further explore this possibility, we expressed WT and D18 N mutant of TREX1 proteins in HEK293T cells and purified them separately. We mixed these two proteins at various ratios and tested their enzyme activity using a linearized plasmid as substrate (Fig. S6). Consistent with previous finding [24,35], WT, but not D18 N mutant of TREX1, has enzymatic activity (Fig. S6C). Mixtures of these two versions of TREX1 also exhibited various levels of activity, depending on the ratios. At 1:1 ratio, the mixture displayed only slightly reduced activity compared to WT TREX1. These results are in line with the absence of cytoplasmic DNA in Trex1$^{WT/D18N}$ MEFs, and strongly support the presence of functional WT/WT homodimers of TREX1 in these cells. It is also possible that differences in the binding affinity to dsDNA between human and mouse *Trex1*D18 N mutants caused the phenotype discrepancy between human and mice carrying D18 N mutations on a single allele of *Trex1* gene. Another factor to consider is that human faces more complex environmental challenges including UV exposure and pathogen infection, while mice are usually maintained in uniformly clean facilities. It would be intriguing to test whether environmental and frequent pathogen challenges would cause more severe phenotypes in *Trex1*$^{WT/D18N}$ mice.

In both *Trex1*$^{-/-}$ [18,19] and *Trex1*$^{D18N/D18N}$ mice, deletion of one allele of *cGas* was nearly sufficient to rescue mice from the disease phenotype. This gene dosage phenomenon suggests both alleles of *cGas* gene have to be expressed to reach a concentration of cGAS protein that is sufficient to trigger the activation of the pathway in response to low concentrations of cytosolic DNA accumulation caused by TREX1 deficiency. The underlying mechanism is intriguing. A recent study demonstrated that the cellular cGAS was activated through a phase separation mechanism [36]. It is likely that concentrations of both DNA and cGAS are critical factors in forming such liquid droplets and thereby "switching on" the signaling pathway. These results raise the interesting possibility that partial inhibition of cGAS activation may be sufficient to alleviate symptoms of autoimmune diseases in patients carrying *TREX1* gene mutations.

4. Materials and methods

4.1. Mice

Trex1$^{D18N/D18N}$ mice were generated by the CRISPR-Cas9 knock-in strategy with previously reported methods [37,38], which introduced the D18 N point mutation into the zygote. Briefly, the Cas9 protein and the D18 N sgRNA were co-injected into the zygotes from C57BL/6 with an 120bp oligo DNA containing the D18 N point mutation sequence. *cGas*$^{-/-}$ mice were created by the CRISPR-Cas9 knockout technology on C57BL/6 background. The sequences of the D18 N and *cGas* single-guide RNA were as follows: sgD18 N CCACTGGCCTGCCTTCGTCT and sg*cGas* CCTTACGACTTTCCGCGCCT. In our studies, male and female mice exhibited similar phenotypes so that they were randomly allocated for all experiments. Mice were bred and maintained under specific pathogen-free conditions in the Animal Center of Fujian Normal University. All research and animal care procedures were approved by the Animal Ethical and Welfare Committee of Fujian Normal University.

4.2. Pathology

All fresh tissues in the studies were fixed in 4% neutral buffered formalin and paraffin embedded, which were then cut into 5−μm section for the staining with hematoxylin and eosin or picrosirius red. The histological analysis of tissues was performed by blind evaluation following the previously described [17].

4.3. Immunofluorescence and immunohistochemistry

For detection of immune complex deposition in the kidneys, fresh tissues were frozen in OCT and stored at −80 °C until sectioning. The kidney tissues were sectioned at 7 μm and fix in acetone. The sections were blocked in PBS with 1% BSA for 1 h and then incubated with anti-mouse IgG Alexa Fluor 488 (Abcam, ab150117). After washing, the section slides were imaged with a Zeiss LSM 780 confocal microscope. For cytoplasmic dsDNA staining, cells were fixed for 15 min in 4% PFA in PBS and permeabilized with 0.1% saponin for 15 min, followed by blocking with 1% BSA, 0.1% saponin in PBS for 1 h and then incubated with anti-dsDNA antibody (Abcam., ab27156) overnight at 4 °C. After three washes, cells were incubated with anti-mouse IgG H&L secondary antibody-Alexa fluor 488 (Invitrogen, A-21202) for 1 h at RT. After washes, the slides were mounted with mounting medium containing Hoechst 33342 (Invitrogen, H3570). For the performance of CD45 and F4/80 staining, kidneys were isolated and fixed in 4% neutral buffered formalin, then the tissues were embedded in paraffin and sectioned. The paraffin-sections were blocked in hydrogen peroxide and incubated with anti-CD45 (Abcam, ab10558) and anti-F4/80 (Abcam, ab6640) antibodies after antigen retrieval. The sections were counterstained with hematoxylin after incubation with diaminobenzidine.

4.4. ELISA

Sera from 4-month-old mice of different genotypes were performed

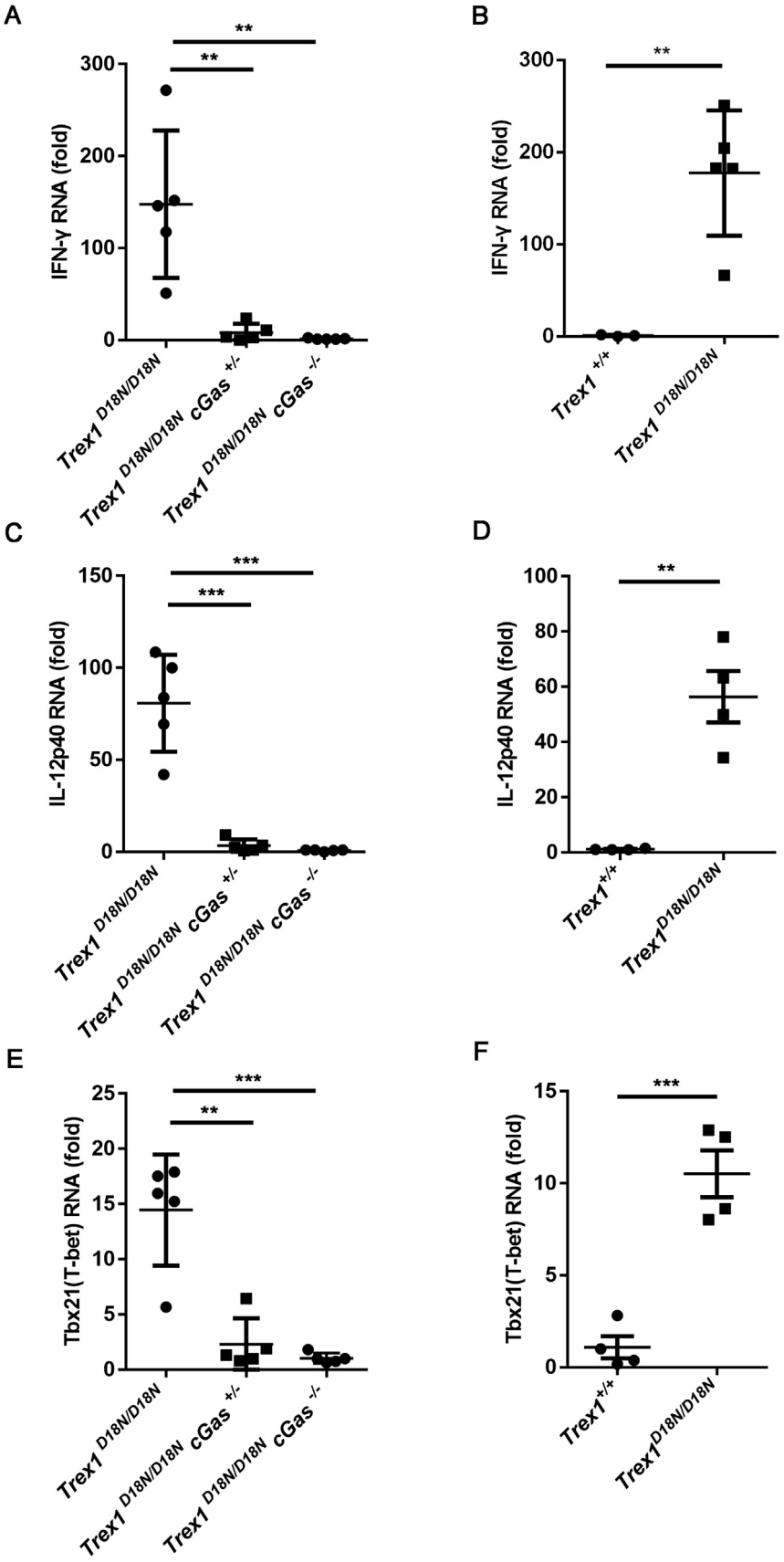

Fig. 6. cGAS mediates infiltration of autoreactive immune cells in the hearts of *Trex1*$^{D18N/D18N}$ mice. Quantitative RT-PCR analysis of IFN-γ (**A** and **B**), IL-12p40 (**C** and **D**) or T-bet (**E** and **F**) RNA in hearts from mice of indicated genotypes. Fold changes are relative to WT (B, D and F) or *Trex1*$^{D18N/D18N}$ *cGas*$^{-/-}$ (A, C and E). Error bars represent SD. *$p < 0.05$; **$p < 0.01$; ***$p < 0.001$; ****$p < 0.0001$, by unpaired Student's *t*-test.

to analyze autoantibodies levels. The levels of autoantibodies were determined by the ELISA kits (Alpha Diagnostics International) according to the manufacturer's instructions. Plasma IL-12 was measured by using the Mouse IL-12 (p70) ELISA Kit (Biolegend) according to the manufacturer's instructions.

4.5. Flow cytometry

Spleens removed from 4-month-old mice were pressed through the cell strainer to collect splenic cells in PBS with 2% FCS (Hyclone). Red blood cells were removed by red blood cell lysing solution. Samples were resuspended in straining buffer (2% FCS in PBS) and cell counts were then performed. For surface staining, samples were incubated with antibody in staining buffer for 30 min at 4 °C. For T regulatory cell staining, splenocytes or PBMCs were treated with 50 ng/mL PMA, 1 μM ionomycin and 1 μg/mL brefeldin A for 4.5 h. And stimulated cells were stained with murine CD3, CD4 and CD8 antibodies. Cells were then treated according to the protocol for Cytofix/Cytoperm™ Fixation/Permeabilization Kit (BD Bioscience). For transcription factor staining, cells were preformed following BD Pharmingen™ transcription factor kit protocol. Samples were analyzed on a FACSymphony™ A5 instrument (BD Biosciences, CA, USA) and data were analyzed using FlowJo software. Antibodies used for staining were as following: CD3-Percp Cy5.5, CD3-BV421,CD4-FITC, CD4-Percp Cy5.5, CD8-APC, CD8-FITC, CD44-APC, CD62L-PE, IFN-γ-PE, T-bet-APC, Ly6c-APC(BD Bioscience).

4.6. Cell culture

Primary MEFs were isolated from day 13.5 embryos of indicated mice. MEFs were maintained in DMEM (Dulbecco's modified Eagle medium) supplemented with 10% FBS (Fetal bovine serum) with the addition of 100 U/ml penicillin and 100 mg/mL streptomycin, and cultured at 37 °C with 5% CO_2. Cells within 5 passages were used for experiments.

4.7. Quantitative real-time PCR and RNA seq

Total RNA of the tissues and cells was isolated with TRIzol reagent (Thermo Fisher Scientific, USA) according to the manufacturer's protocol. cDNA was reversely transcribed by PrimeScript™ RT reagent Kit (Takara). Primers and qPCR analysis was performed as previously described [18]. Quant 6 Flex PCR system (Applied Biosystems, USA) were used for quantitative RT-PCR analysis. Relative expression of the ISGs was normalized by the level of mHPRT expression in each sample. RNA-seq was performed and analyzed as previously described [39].

4.8. Western Blotting

Whole-cell lysates were extracted with cell lysis buffer (20 mM Tris, pH7.5, 150 mM NaCl, 0.5% NP40, 0.2 mM EDTA, 0.2 mM EGTA, 10% glycerol and 1× protease inhibitor cocktail). Proteins were separated by SDS-PAGE then transferred to PVDF membrane (Millipore). Membranes were blocked in 5% non-fat milk in TBS with 0.1% Tween and incubated with antibody against cGAS (Cell Signaling Technology), TREX1 (Santa Cruz) and GAPDH (Sigma-Aldrich).

4.9. Exonuclease assays

The exonuclease assay was performed as previously described [35]. Briefly, FLAG-tagged TREX1 and its mutants were expressed in HEK293T cells and affinity-purified using anti-Flag beads. The TREX1 enzymes were then used to digest linearized PUC19 plasmids in the reaction buffer (20 mM Tris pH 7.5, 5 mM MgCl2, 2 mM DTT, 100 μg/ml BSA) at 25 °C for 30 min. The reaction products were examined by agarose electrophoresis.

Conflicts of interest

The authors declare that there is no conflict of interests regarding the publication of this article.

Author contributions

QC and LS: conception and experimental design, data interpretation, manuscript writing. NX: experimental design, data generation, manuscript writing; JW, SX, MH, KD, SZ: data generation and analysis.

Acknowledgements

We thank Shaoli Cai and Zhang Lin for administrative assistance, Dr. Daliang Li and the laboratory members for technical assistance and helpful discussion. Dr. Kaixin Du (Xiamen Humanity Hospital) for performing the histology analyses of mouse tissues. This study was supported by a grant from Fujian Key Laboratories Funds (2015J1001), Fujian Provincial Industrial Technology Development and Application Project (2016Y0027), and Fujian Bairen Program Funds, Fujian Normal University Key Laboratory Construction Funds, and Fujian Normal University Start-up Funds.

Appendix A. Supplementary data

Supplementary data to this article can be found online at https://doi.org/10.1016/j.jaut.2019.03.001.

References

[1] A. Ablasser, C. Hertrich, R. Waßermann, V. Hornung, Nucleic acid driven sterile inflammation, Clin. Immunol. 147 (2013) 207–215, https://doi.org/10.1016/j.clim.2013.01.003.
[2] S. Pandey, T. Kawai, S. Akira, Microbial sensing by Toll-like receptors and intracellular nucleic acid sensors, Cold Spring Harb. Perspect. Biol. 7 (2014) a016246, , https://doi.org/10.1101/cshperspect.a016246.
[3] T. Kawai, S. Akira, Toll-like receptors and their crosstalk with other innate receptors in infection and immunity, Immunity 34 (2011) 637–650, https://doi.org/10.1016/j.immuni.2011.05.006.
[4] J. Wu, L. Sun, X. Chen, F. Du, H. Shi, C. Chen, Z.J. Chen, Cyclic GMP-AMP is an endogenous second messenger in innate immune signaling by cytosolic DNA, Science 339 (80) (2013) 826–830, https://doi.org/10.1126/science.1229963.
[5] L. Sun, J. Wu, F. Du, X. Chen, Z.J. Chen, Cyclic GMP-AMP synthase is a cytosolic DNA sensor that activates the type I interferon pathway, Science 339 (2013) 786–791, https://doi.org/10.1126/science.1232458 80-.
[6] D. Gao, J. Wu, Y.T. Wu, F. Du, C. Aroh, N. Yan, L. Sun, Z.J. Chen, Cyclic GMP-AMP synthase is an innate immune sensor of HIV and other retroviruses, Science 341 (2013) 903–906, https://doi.org/10.1126/science.1240933 80.
[7] J. Wu, Z.J. Chen, Innate immune sensing and signaling of cytosolic nucleic acids, Annu. Rev. Immunol. 32 (2014) 461–488, https://doi.org/10.1146/annurev-immunol-032713-120156.
[8] Q. Chen, L. Sun, Z.J. Chen, Regulation and function of the cGAS-STING pathway of cytosolic DNA sensing, Nat. Immunol. 17 (2016) 1142–1149, https://doi.org/10.1038/ni.3558.
[9] N. Yan, A.D. Regalado-magdos, B. Stiggelbout, M.A. Lee-kirsch, The cytosolic exonuclease TREX1 inhibits the innate immune response to HIV-1, Nat. Immunol. 11 (2010) 1005–1013, https://doi.org/10.1038/ni.1941 (The).
[10] Y.G. Yang, T. Lindahl, D.E. Barnes, Trex1 exonuclease degrades ssDNA to prevent chronic checkpoint Activation and autoimmune disease, Cell 131 (2007) 873–886, https://doi.org/10.1016/j.cell.2007.10.017.
[11] Y.J. Crow, B.E. Hayward, R. Parmar, P. Robins, A. Leitch, M. Ali, Mutations in the gene encoding the 3′-5′ DNA exonuclease TREX1 cause Aicardi-Goutières syndrome at the AGS1 locus, Nat. Genet. 38 (2006) 917–920, https://doi.org/10.1038/ng1845.
[12] G. Rice, W.G. Newman, J. Dean, T. Patrick, R. Parmar, K. Flintoff, P. Robins, S. Harvey, T. Hollis, A. O'Hara, A.L. Herrick, A.P. Bowden, F.W. Perrino, T. Lindahl, D.E. Barnes, Y.J. Crow, Heterozygous mutations in TREX1 cause familial chilblain lupus and dominant aicardi-goutières syndrome, Am. J. Hum. Genet. 80 (2007) 811–815, https://doi.org/10.1086/513443.
[13] G.I. Rice, M.P. Rodero, Y.J. Crow, Human disease phenotypes associated with mutations in TREX1, J. Clin. Immunol. 35 (2015) 235–243, https://doi.org/10.1007/s10875-015-0147-3.
[14] M.K. Crow, Type I interferon in systemic lupus erythematosus, Curr. Top. Microbiol. Immunol. 316 (2007) 359–386, https://doi.org/10.1007/978-3-540-71329-6-17.
[15] Y.J. Crow, N. Manel, Aicardi-Goutières syndrome and the type I interferonopathies, Nat. Rev. Immunol. 15 (2015) 429–440, https://doi.org/10.1038/nri3850.

[16] A.T. Reder, X. Feng, Aberrant type I interferon regulation in autoimmunity: opposite directions in MS and SLE, shaped by evolution and body ecology, Front. Immunol. 4 (2013), https://doi.org/10.3389/fimmu.2013.00281.
[17] A. Gall, P. Treuting, K.B. Elkon, Y.M. Loo, M. Gale, G.N. Barber, D.B. Stetson, Autoimmunity initiates in nonhematopoietic cells and progresses via lymphocytes in an interferon-dependent autoimmune disease, Immunity 36 (2012) 120–131, https://doi.org/10.1016/j.immuni.2011.11.018.
[18] D. Gao, T. Li, X.-D. Li, X. Chen, Q.-Z. Li, M. Wight-Carter, Z.J. Chen, Activation of cyclic GMP-AMP synthase by self-DNA causes autoimmune diseases, Proc. Natl. Acad. Sci. Unit. States Am. 112 (2015) E5699–E5705, https://doi.org/10.1073/pnas.1516465112.
[19] E.E. Gray, P.M. Treuting, J.J. Woodward, D.B. Stetson, Cutting edge: cGAS is required for lethal autoimmune disease in the trex1-deficient mouse model of aicardi–goutières syndrome, J. Immunol. 195 (2015) 1939–1943, https://doi.org/10.4049/jimmunol.1500969.
[20] J.L. Grieves, J.M. Fye, S. Harvey, J.M. Grayson, T. Hollis, F.W. Perrino, Exonuclease TREX1 degrades double-stranded DNA to prevent spontaneous lupus-like inflammatory disease, Proc. Natl. Acad. Sci. Unit. States Am. 112 (2015) 5117–5122, https://doi.org/10.1073/pnas.1423804112.
[21] S.L. Rego, S. Harvey, S.R. Simpson, W.O. Hemphill, Z.A. McIver, J.M. Grayson, F.W. Perrino, TREX1 D18N mice fail to process erythroblast DNA resulting in inflammation and dysfunctional erythropoiesis, Autoimmunity (2018) 1–12, https://doi.org/10.1080/08916934.2018.1522305.
[22] Y. Obata, T. Tanaka, E. Stockert, R.A. Good, Autoimmune and lymphoproliferative disease in (B6-GIX+ X 129)F1 mice: relation to naturally occurring antibodies against murine leukemia virus-related cell surface antigens, Proc. Natl. Acad. Sci. U. S. A 76 (1979) 5289–5293, https://doi.org/10.1073/pnas.76.10.5289.
[23] D. Kavanagh, D. Spitzer, P.H. Kothari, A. Shaikh, M.K. Liszewski, A. Richards, J.P. Atkinson, New roles for the major human 3′-5′ exonuclease TREX1 in human disease, Cell Cycle 7 (2008) 1718–1725, https://doi.org/10.4161/cc.7.12.6162.
[24] D.A. Lehtinen, S. Harvey, M.J. Mulcahy, T. Hollis, F.W. Perrino, The TREX1 double-stranded DNA degradation activity is defective in dominant mutations associated with autoimmune disease, J. Biol. Chem. 283 (2008) 31649–31656, https://doi.org/10.1074/jbc.M806155200.
[25] J.R. Giles, M. Kashgarian, P.A. Koni, M.J. Shlomchik, B cell–specific MHC class II deletion reveals multiple nonredundant roles for B cell antigen presentation in murine lupus, J. Immunol. 195 (2015) 2571–2579, https://doi.org/10.4049/jimmunol.1500792.
[26] D.B. Stetson, J.S. Ko, T. Heidmann, R. Medzhitov, Trex1 prevents cell-intrinsic initiation of autoimmunity, Cell 134 (2008) 587–598, https://doi.org/10.1016/j.cell.2008.06.032.
[27] G. Rice, T. Patrick, R. Parmar, C.F. Taylor, A. Aeby, J. Aicardi, P. Lebon, Clinical and molecular phenotype of aicardi-goutières syndrome, Am. J. Hum. Genet. 81 (2007) 713–725, https://doi.org/10.1086/521373.
[28] B. de Vries, G.M. Steup-Beekman, J. Haan, E.L. Bollen, J. Luyendijk, R.R. Frants, G.M. Terwindt, M.A. van Buchem, T.W.J. Huizinga, A.M.J.M. van den Maagdenberg, M.D. Ferrari, TREX1 gene variant in neuropsychiatric systemic lupus erythematosus, Ann. Rheum. Dis. 69 (2010) 1886–1887, https://doi.org/10.1136/ard.2009.114157.
[29] M.A. Lee-Kirsch, M. Gong, H. Schulz, F. Rüschendorf, A. Stein, C. Pfeiffer, A. Ballarini, M. Gahr, N. Hubner, M. Linné, Familial chilblain lupus, a monogenic form of cutaneous lupus erythematosus, maps to chromosome 3p, Am. J. Hum. Genet. 79 (2006) 731–737, https://doi.org/10.1086/507848.
[30] K.W. Huang, T.C. Liu, R.Y. Liang, L.Y. Chu, H. Lo Cheng, J.W. Chu, Y.Y. Hsiao, Structural basis for overhang excision and terminal unwinding of DNA duplexes by TREX1, PLoS Biol. 16 (2018), https://doi.org/10.1371/journal.pbio.2005653.
[31] M.A. Lee-Kirsch, D. Chowdhury, S. Harvey, M. Gong, L. Senenko, K. Engel, C. Pfeiffer, T. Hollis, M. Gahr, F.W. Perrino, J. Lieberman, N. Hubner, A mutation in TREX1 that impairs susceptibility to granzyme A-mediated cell death underlies familial chilblain lupus, J. Mol. Med. 85 (2007) 531–537, https://doi.org/10.1007/s00109-007-0199-9.
[32] M. Hasan, C.S. Fermaintt, N. Gao, T. Sakai, T. Miyazaki, S. Jiang, Q.Z. Li, J.P. Atkinson, H.C. Morse, M.A. Lehrman, N. Yan, Cytosolic nuclease TREX1 regulates oligosaccharyltransferase activity independent of nuclease activity to suppress immune activation, Immunity 43 (2015) 463–474, https://doi.org/10.1016/j.immuni.2015.07.022.
[33] M. Kucej, C.S. Fermaintt, K. Yang, R.A. Irizarry-Caro, N. Yan, Mitotic phosphorylation of TREX1 C terminus disrupts TREX1 regulation of the oligosaccharyltransferase complex, Cell Rep. 18 (2017) 2600–2607, https://doi.org/10.1016/j.celrep.2017.02.051.
[34] T. Sakai, T. Miyazaki, D.M. Shin, Y.S. Kim, C.F. Qi, R. Fariss, J. Munasinghe, H. Wang, A.L. Kovalchuk, P.H. Kothari, C.S. Fermaintt, J.P. Atkinson, F.W. Perrino, N. Yan, H.C. Morse, DNase-active TREX1 frame-shift mutants induce serologic autoimmunity in mice, J. Autoimmun. 81 (2017) 13–23, https://doi.org/10.1016/j.jaut.2017.03.001.
[35] J.M. Fye, C.D. Orebaugh, S.R. Coffin, T. Hollis, F.W. Perrino, Dominant mutations of the TREX1 exonuclease gene in lupus and aicardi-goutières syndrome, J. Biol. Chem. 286 (2011) 32373–32382, https://doi.org/10.1074/jbc.M111.276287.
[36] M. Du, Z.J. Chen, DNA-induced liquid phase condensation of cGAS activates innate immune signaling, Science 361 (2018) 704–709, https://doi.org/10.1126/science.aat1022 80-.
[37] T. Aida, K. Chiyo, T. Usami, H. Ishikubo, R. Imahashi, Y. Wada, K.F. Tanaka, T. Sakuma, T. Yamamoto, K. Tanaka, Cloning-free CRISPR/Cas system facilitates functional cassette knock-in in mice, Genome Biol. 16 (2015), https://doi.org/10.1186/s13059-015-0653-x.
[38] H. Wang, H. Yang, C.S. Shivalila, M.M. Dawlaty, A.W. Cheng, F. Zhang, R. Jaenisch, One-step generation of mice carrying mutations in multiple genes by CRISPR/cas-mediated genome engineering, Cell 153 (2013) 910–918, https://doi.org/10.1016/j.cell.2013.04.025.
[39] K.J. Mackenzie, P. Carroll, L. Lettice, Ž. Tarnauskaitė, K. Reddy, F. Dix, A. Revuelta, E. Abbondati, R.E. Rigby, B. Rabe, F. Kilanowski, G. Grimes, A. Fluteau, P.S. Devenney, R.E. Hill, M.A. Reijns, A.P. Jackson, Ribonuclease H2 mutations induce a cGAS/STING-dependent innate immune response, EMBO J. 35 (2016) 831–844, https://doi.org/10.15252/embj.201593339.